Proceedings World Geothermal Congress 2015
Melbourne, Australia, 19-25 April 2015

Geothermal Exploration Where Innovative Meets Classic Geothermal Exploration in Western Anatolia

Eric Klingel, Metin Tavlan, Kivanc Ozcetin and Charlotte de Wijkerslooth

Keywords: Exploration, MMR gas sampling, structural mapping

ABSTRACT

The exploration process for a geothermal play in western Anatolia was to integrate new and classic geothermal exploration techniques to determine exploratory slim hole locations. The new method is the use of magmatic, mantle, and radiogenic (MMR) gas exploration method to determine the temperature, relative depth, type of geothermal source, and the classic method is detailed structural and petrological mapping over the area selected by the MMR exploration.

The MMR gas exploration method was the first technique used to reduce the size of the geothermal play from forty five square kilometers to an inferred geothermal resource of approximately four square kilometers. The MMR gas sampling and analysis procedure is a shallow invasive geothermal exploration procedure designed to assist in identifying geothermal play, taking it to development stages, or determining that it does not exist. The procedure follows established work in volcanic research, soil vapor environmental surveys and mineral exploration techniques. The MMR gas survey takes gas samples in potential geothermal play areas from an average depth of one to three meters by using driven soil gas probes and prepared custom samples bottles and/or copper tubes. The collected gas is then analyzed for MMR gases CO_2, Ar, CO, N_2, He, O_2 H_2S, H_2, CH_4, and select gas isotopes. Using gas concentrations, gas ratios and gas isotopes, certain factors can be determined to assist identifying the geothermal resource. The geothermal factors determined are listed below in order of difficulty of interpretation:

1. Presence or absence of MMR gases of magmatic origin
2. Differentiation between non-magmatic and magmatic source of MMR gases
3. Estimated temperature of thermal energy in place
4. MMR gas quantitative comparisons may indicate areas of effective porosity, either fracture or porous media porosity
5. Geometry and/or location of geothermal source
6. Relative depth to thermal energy in place
7. Grouping or contouring the MMR gas concentrations in conjunction with the above data may provide improved placement of temperature gradient and slim hole exploration wells and surface geophysical work.

The MMR gas survey took 37 gas samples in areas with potential thermal energy in place. The collected gases were then analyzed for CO_2, CH_4, CO, He, N_2, H_2S, O_2, and H_2 and, using comparative gas geothermometers, temperatures of potential geothermal sources were determined. The MMR gas exploration method found the highest area of concentration of intermediate to deep MMR gas temperatures in a four square kilometer area in the southeastern area of the Concession and ranged from 107º to 139ºC and 207º to 239ºC, respectively.

Structural and petrological mapping was done in detail to pick up where MMR exploration identified details in rugged terrain that would further reduce the areas for exploration slim holes. Local lithologies have been mapped as an overlay on the current geological map such as fault breccia/gouge and abrupt changes in lithology that may indicate offset or dilation. From the field measurements, stereo net projections were performed for a series of joint patterns to determine minor fractures and their association with the major faults trends. The mapping did confirm that the reduced area of the inferred geothermal resource corresponds to the intersection of two fault sets: (i) NE–SW trending oblique faults and (ii) WNW–ESE trending normal faults. The first fault set was active during Miocene forming/deforming the Selendi Graben and its sedimentary fills; whilst the latter is still active as its southern major conjugate is the Gediz Graben System. Additionally, the world stress map suggests a NW–SE orientation for the youngest tectonic activity (which in turn are open fractures that transmit fluids) in the region based on two SH azimuth measurements (maximum horizontal stress) of 125 and 101 degrees.

1. INTRODUCTION

The evolution of active geothermal systems in Western Anatolia goes to back to pre-Neotectonic fossil geothermal systems. The active geothermal systems of Early Miocene which are now fossil geothermal systems of Quaternary have been evaluated as volcanic-magmatic heat sources. The present day geothermal systems have changed and are tectonic-magmatic heat sources (Tokcaer and Savascin, 2007). These tectonic-magmatic heat sources are deep seated in the lower crust and upper mantle and have limited surface expression for geothermometry determination, but have sufficient surface fracture and petrographical outcrops for structural and geologic mapping.

Much of western Turkey has undergone significant north-south extension from early Miocene to Recent time (Isik et al., 2003). Variation in chemistry of the volcanic rocks closely parallels this Miocene to Recent Tectonic evolution. Subduction of the African plate under western Anatolia was responsible for the widespread andesitic volcanism of early Miocene time. The change of dominantly dacitic and ignimbrite eruptions may have been a result of continental crust input. This area was characterized during early Miocene time by an anomalously thick crust in north–south compression (Figure 1).

The collision of the Arabian Platform with eastern Anatolia and Iran was immediately mirrored by a compositional change in western Anatolian volcanic rocks. An extensional environment replaced the prior compressional regime in western Anatolia as movement began along the north and south Anatolian transform faults (extension). Lavas of the Anatolia region in this transitional

period were of highly complex origin, with both crust and mantle sources (Faulds, 2009 and Dyer, 1987). Continuous extension and widespread thinning of the lithosphere facilitated rapid ascent of basaltic magmas without much residence time in the crust and hence the eruption of relatively uncontaminated asthenosphere-derived magmas at the surface (i.e., Kula lavas in western Anatolia).

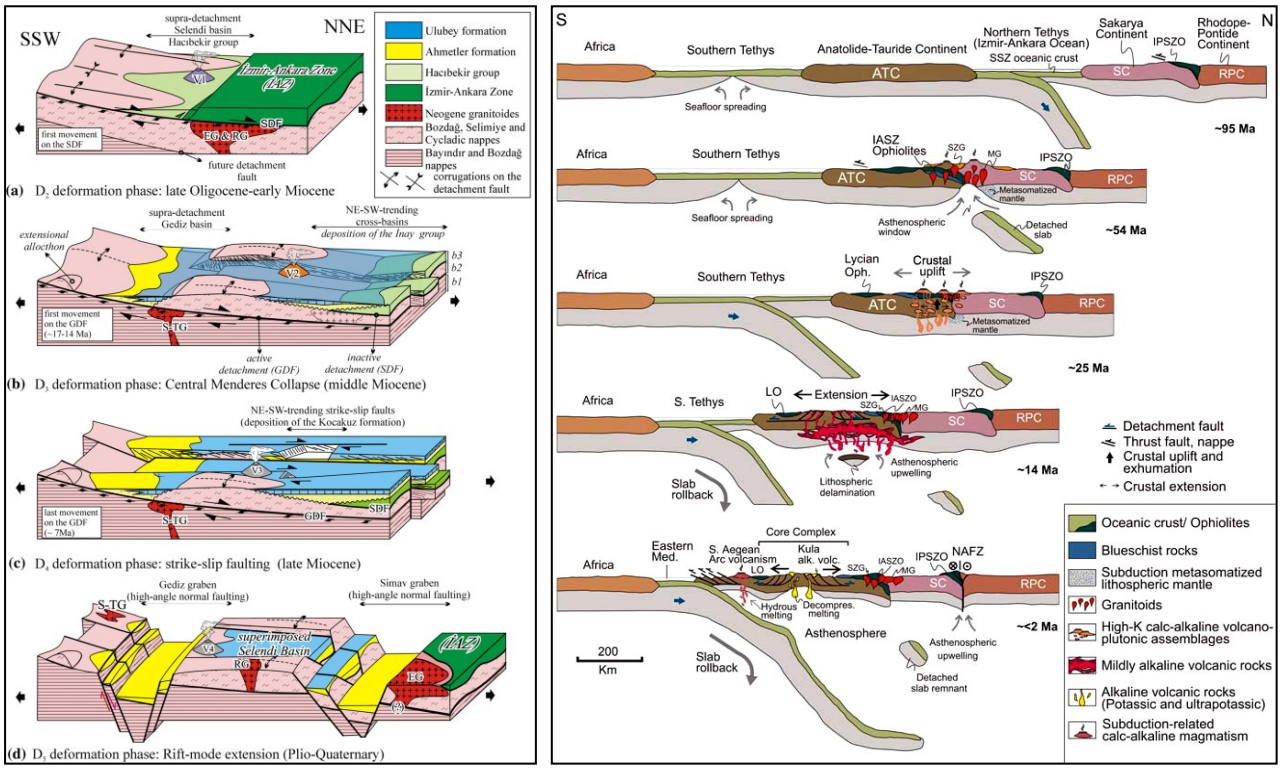

Figure 1: Left; Deformational history of Kula Region (adapted from Ersoy and others 2010) and right; Late Mesozoic–Cenozoic geodynamic evolution of the western Anatolian orogenic belt through collision and extensional processes in the upper plate of north-dipping subduction zone(s) within the Tethyan realm (adapted from Dilek, 2009).

From late Miocene to Recent time, much smaller isolated magmatic centers were present. The amount of volcanism may be a direct function of available water to generate melts; therefore activity would have been more abundant during active subduction in early Miocene time (Dilek and Altunkaynak, 2006) (Figure 1). Also, the development of the present horst and graben terrain, with lystric surfaced normal faults may have impeded magma migration through the crust. The occurrence of nearly all young volcanic centers and thermal springs in the Kula area at the intersection of fault trends supports these intersections as the only path for the magmas (Ersoy and others 2010).

Many of the geothermal systems in this region lie within or along the margins of major east-west trending grabens, which are bounded by major low angle detachment faults and / or steeply dipping normal fault systems. Recent magmatism in the region has been limited to the Quaternary alkaline basalts of the Kula volcanic field, set between the Gediz and Simav grabens (Figure 2). Isotopic and trace–element compositions within these basalts indicate derivation primarily from asthenospheric mantle, with a limited lithospheric mantle contribution and essentially no crustal contamination (Alici et al., 2002). Although proximal to several geothermal fields, the deep sources for the Kula basalts indicate that related magmas do not provide a direct source of heat for these geothermal systems.

To conduct geothermal exploration in the partially blind region of the recent Quaternary magmatism of the Kula volcanic fields and surrounding area in western Anatolia it was necessary to integrate innovative and classic geothermal exploration techniques to determine exploration slim hole locations. The innovative exploration methods was the use of magmatic, mantle, and radiogenic (MMR) gas exploration methodology to determine the temperatures, relative depth and type of geothermal source, and the classic exploration methodology was to determine the fracture permeability and potential reservoirs using detailed structural and petrological mapping over the area with the most promising temperature anomalies determined by the MMR exploration.

2. MMR GAS EXPLORATION METHODOLOGY

The MMR gas sampling and analysis procedure is a shallow invasive geothermal exploration procedure designed to assist in identifying geothermal play, taking it to development stages, or determining that it does not exist. The procedure follows established work in volcanic research, soil vapor environmental surveys and mineral exploration techniques. The MMR gas survey takes gas samples in potential geothermal play areas from an average depth of one to three meters by using driven soil gas probes and prepared custom samples bottles and/or copper tubes. The collected gas is then analyzed for MMR gases CO_2, Ar, CO, N_2, He, O_2 H_2S, H_2, CH_4, and select gas isotopes. Using gas concentrations, gas ratios and gas isotopes, certain factors can be determined to assist identifying the geothermal resource. The geothermal factors determined are listed below in order of difficulty of interpretation:

1. Presence or absence of MMR gases of magmatic origin
2. Differentiation between non-magmatic and magmatic source for MMR gases
3. Estimated temperature of thermal energy in place
4. MMR gas quantitative comparisons may indicate areas of effective porosity, either fracture or porous media porosity
5. Geometry and/or location of geothermal source
6. Relative depth to thermal energy in place
7. Grouping or contouring the MMR gas concentrations in conjunction with the above data analysis may provide improved placement of temperature gradient and slim hole exploration wells and surface geophysical work.

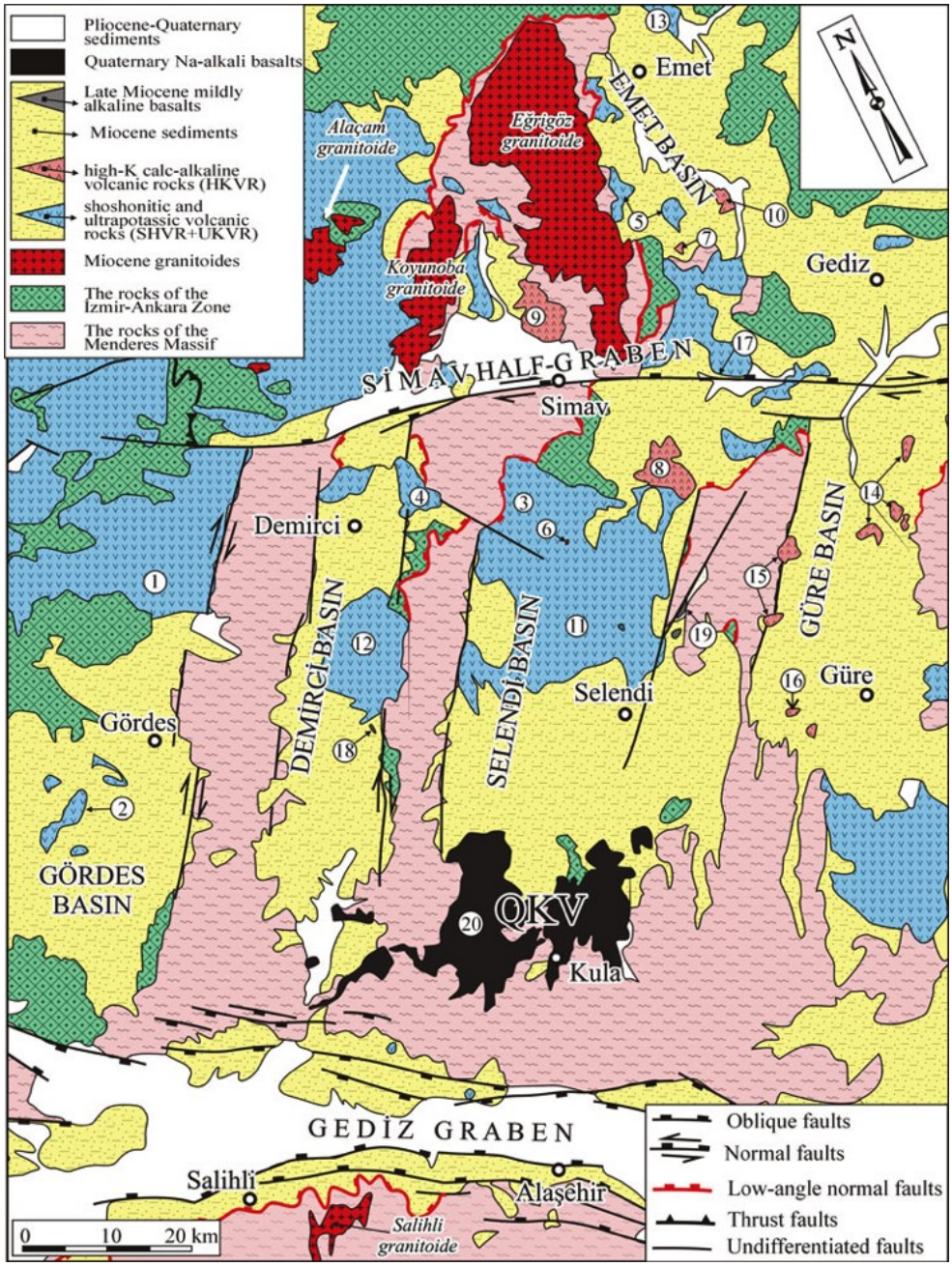

Figure 2: Generalized geological map of the ne-sw trending basins between the Gediz Graben and the Simav Half Graben. NOTE: the north arrow direction. Adapted from Ersoy, 2012.

Sampling points that did not follow the grid pattern distribution for the Kula Concessions were chosen based on the following individually weighted subjects:

- Geology (stratigraphy, structural geology, petrology, geochemistry, tectonics and heat flow)
- Presence of geothermal indicators,
- Accessibility in terms of drilling and sampling,

Selected MMR points that did not follow the grid pattern distribution were chosen, because of the presence of geothermal indicators, accessibility and geology within the Kula Concessions. In the area of the Kula Concessions thirty seven MMR gas sampling locations were identified (Figure 3). Sample density was based on having sufficient sample points to cover the concessions allowing for non-usable points.

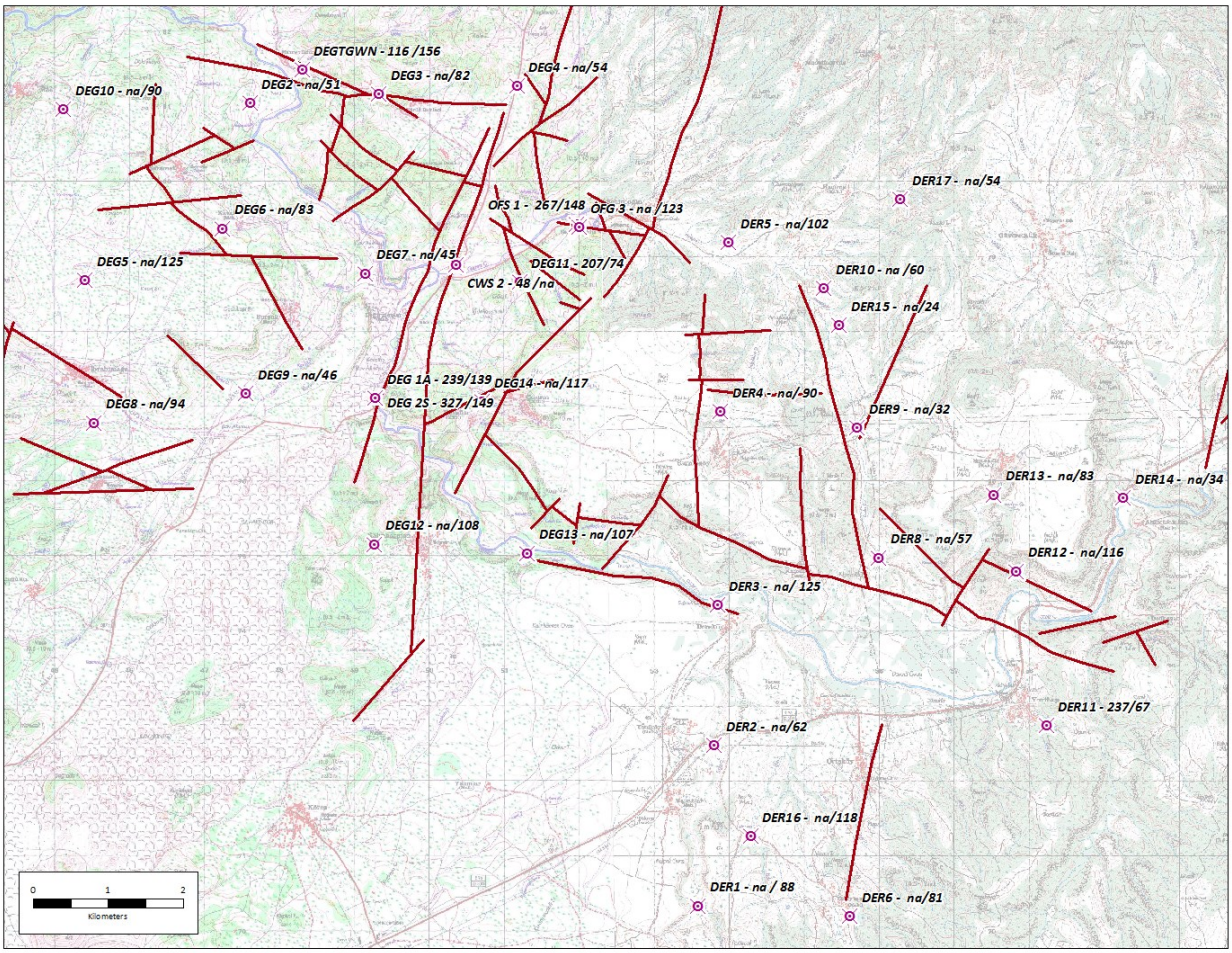

Figure 3: Thirty seven MMR gas sampling locations and fault data in the Kula region

The MMR gas exploration method was used first to reduce the size of the geothermal play from forty five square kilometers to an inferred geothermal resource of approximately four square kilometers. The MMR gas survey took 37 gas samples in suspected areas of thermal energy in place. The collected gases were then analyzed for CO_2, CH_4, CO, He, N_2, H_2S, O_2, and H_2 and using comparative gas geothermometers temperatures of potential geothermal sources were determined

The sampling grid was large and included areas that were to be used as background points.

MMR gas samples were taken following these steps:

- Where competent rock was encountered create a three quarter inch diameter hole using a Rotary hammer drill to a maximum depth of one meter (Photo 1).
- Continue the pilot hole by driving a solid five eighths inch diameter steel rod with a hammer drill or slide hammer to a maximum of three meters below ground surface or rod refusal to create a pilot hole for the gas recovery rod.
- Where unconsolidated regolith is encountered the pilot hole was created solely by hammer drilling solid rods.
- Remove the solid rods.
- Drive a hollow gas recovery point and rod with tubing attached to the gas recovery point into the pilot hole with a hammer drill (Photo 2).
- Seal the bore hole annulus to reduce atmospheric air contamination.
- Attach the tubing to a copper tube sampler or Giggenbach sample bottle.
- Purge the air out of the tubing, copper tube or Giggenbach bottle and annulus (Photo 3).
- Allow gas to enter copper tube or Giggenbach bottle.
- Seal off the copper tube by cold welding the ends of the copper tube or close the Giggenbach bottle seal.
- Remove the hollow rods and seal the bore hole.

Photo 1: Rotary hammer drilling and hammering to create pilot for hollow rods

Photo 2: Placement of hollow rods and gas collection tubing

Photo 3: Collection of MMR Gas Sample in Giggenbach Bottle

MMR gas samples collected in glass sampling bottles and/or copper tubes are then analyzed in the Volcanic and Hydrothermal fluids laboratory at the University of New Mexico in the Department of Earth and Planetary Sciences. The analytical system consists of two instruments connected to a high vacuum system. The first instrument is a Pfeiffer Quadrupole Mass Spectrometer (QMS) with mass range 0 to 120 AMU. This instrument is used for the elemental analyses of He, Ar, N_2 and O_2 using Secondary Electron Measurement (SEM) and operated in dynamic mode. The second instrument is a Gow Mac gas chromatograph (GC) equipped with a Discharge Ionization Detector (DID), HayeSep D and Molesieve columns and run with ultra-pure and purified helium carrier gas. The GC is used for the elemental analyses of N2, Ar+O2, H2, CO2, CH4, CO. Calibration of both instruments is performed using calibration gas mixtures purchased from Air Liquide. Calibration gas mixtures have an analytical accuracy of ± 5%. Except for low-level (few 10's of ppm) helium, the QMS has a precision of better than 0.1 % for all species. The precision of the GC has not been systematically determined but based on repeated measurements is ± 2 %. The vacuum system consists of high accuracy MKS baratron gauges (total range is ambient to 10-5 torr), a Bayer-Alpert (ion) gauge, a diffusion pump and a roughing pump to back the diffusion pump and to obtain low vacuum. The QMS is connected to a turbo pump that is backed with a second roughing pump. The design of the vacuum line ensures low blanks due to 10-5 torr line pressure and highly accurate calibrations due to the large range of the two MKS Baratron gauges.

3. STRUCTURAL AND PETROGRAPHIC GEOLOGIC EXPLORATION METHODOLOGY

Prior to any kind of (field) exploration survey, the available pre-published information will be gathered and compiled into one database.

Before commencement of the actual fieldwork, geological and lineament maps are produced using Terra-Aster images. Lineaments are any linear features that can be picked out as lines in satellite imagery. Geological features such as faults, joints or boundaries between stratigraphic formations may form such linear trends.

Following that, a more advanced technique – Interferometric synthetic aperture radar (InSAR) - is applied for the detailed analysis of the active structural pattern of the region. InSAR allows accurate measurements of the radiation travel path. Measurements of travel path variations as a function of the satellite position and time of acquisition allow generation of Digital Elevation Models (DEM) and measurement of surface deformations of the terrain at a centimeters scale (Ferretti et al. 2007). InSAR uses two or more SAR images to generate maps of surface deformation. Envisat ASAR ascending track 472 and Envisat ASAR descending track 336 are used in Kula project.

A detailed geological map of the area is produced using the traditional field mapping method where all findings are recorded in the field notebook and topographic base map. At each stop, the location is recorded, rock type described, tectonic features and deformation markers determined and, when necessary, placed in the photographic record.

4. MMR GAS EXPLORATION FINDINGS

Gas samples were analyzed for CO_2, CH_4, CO, N_2, Ar, O_2, He, and H_2 contents. Detection limits vary depending on the gas species. For those species used in geothermometer calculations, i.e., CO_2, H_2, CH_4, CO, N_2, Ar the detection limits are given and are based on peak areas that are detectable by the instrument software.

The majority of samples have high air content as expected with MMR sampling techniques and a very narrow N_2 content of 76 to 78%, O_2 contents from 21 to 22%, and Ar contents from 0.9 to 1%. There are, however, several samples that are distinctly different from air, soil gas sample DEG 1A (81% N_2 and 3.4% O_2); water/gas head space sample GUL-5 (95% N_2 and only 0.13% O_2). In thermal spring and well gas samples N_2 contents range from 81.7% to 0.004% and O_2 contents range from 19% to 0.013% (BAS-1, OFS-1, DEG-S2); two well samples, KES-01 and DEG-TGWM, have non air like levels of N_2 and O_2 with 91.4% N_2 and 7% O_2 and 63% N_2 and 9.5% O_2, respectively. Several thermal spring gas samples also have lower than air (0.9%) Ar contents. Clearly the samples with low O_2, higher or lower than air N_2 and lower than air Ar contents are the best candidates for representing more pristine, i.e., uncontaminated gases that ascend from depth. In the majority of copper tube soil gas samples the CO_2 contents are less than 1%. The highest CO_2 content of any soil gas sample is DEG-1A with 13.8% and a number of samples contain 1-5% CO_2, clearly above the air value of 400 ppm. Gas samples from thermal springs and wellbores have the highest CO_2 contents from 17 to 45% with one well sample (KES-01) at < 1%. It is notable that the majority of samples contain relatively high CO (10 to 126 ppm), with the highest amount sampled by DEG-1A. These samples also contain O_2 in concentrations similar to the atmosphere (21%), implying that O_2 was not consumed by oxidation of CO to CO_2 (which would be a high temperature process). Methane (CH_4) contents of all soil gas samples are lower than the CO contents and below the detection limit for most samples. The situation is reversed in the spring samples, where CH_4 contents are higher than the CO contents and in most samples CO is not detected. Hydrogen contents range from below detection limit to about 500 ppm (DEG-1A) and helium contents range from detection limit to about 91 ppm with most of the highest values occurring in the soil gas samples. Similarly to CO_2, CH_4 in these systems is either derived from a hydrothermal component or from shallow organic matter in sediments. If we discount shallow organic matter, given that soil development is rather limited in this arid region, CH_4 is likely a hydrothermal gas component.

The log (CH_4/CO_2) values of the samples that contain CH_4 range from -0.68 to –4.17 and are generally in the range observed in hydrothermal systems that have gases in equilibrium with a liquid or vapour phase. However, the log (CO/CO_2) values of these samples ranges from -0.83 to – 3.79 which is significantly higher than what has been observed in vapour discharging from hydrothermal systems. The CO_2/He versus N_2/He plot (Diagram 1) allows for the identification of air versus mantle and crustal sources. Air has a CO_2/He ratio of 72, upper mantle derived gases range from 10,000 to 70,000, i.e., Fischer et al. (2009), and typical crustal gases are > 100,000 (O'Nions and Oxburgh, 1988). Spring gas samples and soil gas samples from the DRG concession generally show the highest crustal contributions with possible mantle influence. A number of samples have N_2/He and CO_2/He values that are lower than air, suggesting that CO_2 is affected by precipitation of calcite in the subsurface, i.e. Ray et al. (2009). The $^3He/^4He$ values of spring gases sampled in the Kula region are 2.8 R_A (Gulec et al., 2002), indicating a significant

mantle helium input (upper mantle $^3He/^4He$ is 8±1 R_A, Graham, 2002). Helium concentrations are highest in the Degirmenler Concession, with the highest values at DEG-1A and DEG-7. Both of these localities are located very close to a recent lava flow and on the surface expression of a fault. DEG-1A also has the highest CO_2, CO, and CH_4 contents, and is therefore the best candidate for application of geochemical gas geothermometers to estimate deep equilibrium temperatures.

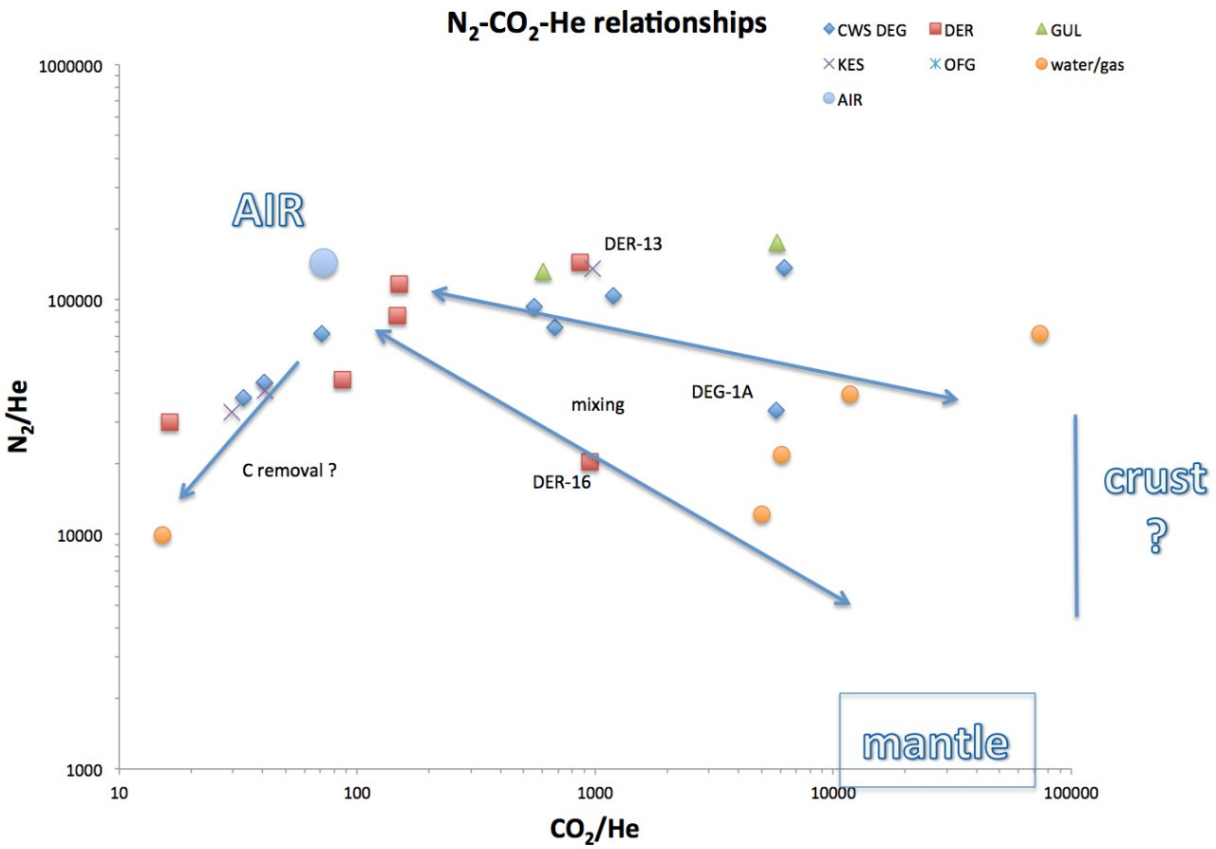

Diagram 1: N_2-CO_2-He relationships of samples collected and potential end members.

In summary, samples have quite variable compositions and contents (N_2, Ar and O_2). CO_2 contents reach up to 13% in soil gas samples and especially noteworthy are the high CO contents which imply a rather reduced environment – in all samples CO is more abundant than CH_4. Gas ratio relationships and helium isotopes from earlier works suggest that these gases are a mixture between air and crustal components with some mantle influence. This interpretation is consistent with the source of volcanism in the region which has an asthenospheric mantle and subcontinental lithospheric mantle affinity (Dyer, 1987; Alici et.al. 2002). Mantle derived gases would move upward through the crust where they pick up additional N_2, CO_2 and He resulting in elevated CO_2/He and N_2/He ratios (Diagram 1). Some of the CO_2 may also be precipitated in the crust leading to lower CO_2/He ratios. CH_4 is of crustal origin. The high CO contents are very unusual and attest to a very reduced source which is typically only encountered in gases discharging from very reduced systems in connection with rift or plume volcanism such as for example in the Afar Region of Northern Africa. The nature of such high reduced carbon compositions in soil gases has not yet been extensively documented and requires further investigation.

5. STRUCTURAL AND PETROLOGICAL FINDINGS

Structural and petrological analyses were performed to pick up where the MMR exploration left off, specifically to identify details in rugged terrain that would further reduce the areas for exploration slim holes.

Field observations agree with the regional stratigraphic model proposed by Ersoy et al. (2010). In summary, four formations were defined in the study area; the Menderes Massif, Hacibekir Group, Inay Group and Basaltic lava flows. The basement of the region is composed by Menderes Massif; primarily consisting of gneiss and schist. The Hacıbekir Group is composed of serpentinite blocks that are encompassed in a clastic matrix overlying the Menderes Massif with angular unconformity. The Menderes Massif was exhumed along the detachment fault zones, and intensively sheared ophiolite slabs broke off into the Yeniköy formation. The Yeniköy Formation (which is the detritic member of Hacıbekir Group) was deformed very intensely in early Miocene. Detachment ends in the middle Miocene and lacustrine environment becomes stagnant. The Inay Group overlies both the Hacıbekir Group and the Menderes Massif with an angular unconformity. Quaternary Kula volcanics have three different eruption phases and overlie all units with an angular unconformity. The ß1 and ß2 eruption phases display characteristic columnar jointing, whereas the ß3 lava flows are characteristically AA lavas. All basalts have asthenospheric origin and instead of observing basaltic composition at the field, they are characteristic with highly alkaline tephritic and phonolitic rocks as geochemically (Ersoy et al., 2011).

In the structural mapping campaign, a number of faults were defined and their orientations measured. Generally, the mapping confirmed that the reduced area of the inferred geothermal resource is host to the intersection of two major fault sets: (i) NE–SW trending oblique faults and (ii) WNW–ESE trending normal faults. The first fault set was active during Miocene forming/deforming the Selendi Graben and its sedimentary fills (Figure 1); whilst the latter is still active as its southern major conjugate is the Gediz Graben System.

Stereonet projection of 48 strike and dip measurements of fault planes and fractures are done to understand how these structural elements are related to the major trends of the region. Resulting patterns and Rose Diagram show NNE-SSW, NW-SE and WNW-ESE trends proving the findings of the desktop studies with the field measurement (Figure 4).

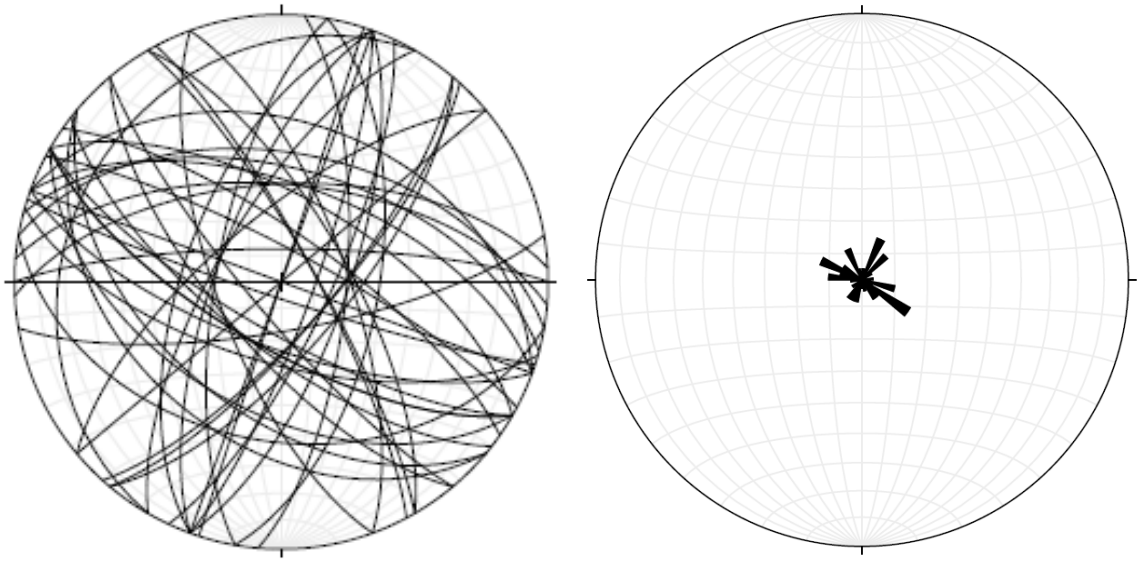

Figure 4: Stereonet projection and rose diagram of 48 fault and fracture plane measurements.

In an effort to link the observed structural features to the present-day stress regime, the world stress map data has been consulted. Two data points have been recorded in the near vicinity of the Kula area, with maximum horizontal compressive stress orientations of 125 and 101 degrees. Theoretically, the fractures parallel to the maximum horizontal compressive stress are preferential for fluid flow as they are subject to the lowest normal stresses. While this is not always the case (chemical alteration can close pathways), it is a good indicator to link to the field- and remote sensing data. Based on the stress measurements, the faults in NW-SE orientation around Kula are probably transmitting fluids. Additionally, the InSAR studies indicate a maximum subsidence rate of 0.2~0.3 cm/yr in Kula denoted by a WNW-ESE trend.

All of these structural findings coincide with the NW–SE trend of the Quaternary Kula volcanics centres.

6. EXPLORATION CONCLUSIONS

6.1 MMR Gas Exploration Conclusions

Gas geothermometers rely on chemical equilibrium processes occurring in the hydrothermal water or steam phase and assume that gas species measured at the surface are derived from such a hydrothermal liquid or gas phase. The application further assumes that the pertinent gas ratios (i.e., CO_2/CH_4) remain unchanged during shallow level processes such as precipitation, partitioning into shallow ground water or contributions from shallow organic sources. Therefore, one needs to be cautious when assigning species that can be derived from shallow organic sources (CO_2 and CH_4) to the hydrothermal phase. For example the CO_2-CH_4 geothermometer of Norman and Bernhardt (1981) relies on CO_2/CH_4 ratios measured in the gas phase and a higher CO_2/CH_4 ratio results in higher temperatures. This is because CO_2 is considered a deep magmatic, high temperature gas component and CH_4 a shallow, lower temperature hydrothermal gas. For example, magmatic high temperature fumaroles contain almost no CH_4 but high $CO2$ (Fischer, 2008) and resulting CO_2-CH_4 temperatures would be magmatic (> 700°C). This is contrary to hydrothermal systems that have high CH_4 contents relative to CO_2 and would give much lower temperatures than the volcanic example.

In the samples from the Deg/Deg Concessions CO_2 contents of soil gas samples vary widely from essentially air-like contents to 14%. In most samples CH_4 is below detection limit, impeding the application of the CH_4-CO_2 geothermometers.

The low CO_2 contents measured in some samples may also be the result of calcite precipitation at depth. Oxidation of CO and CH_4 due to the abundant O_2 measured in the samples would lower the CO and CH_4 contents of the samples, although the O_2 contents are similar to air values in the majority of samples and there does not seem to have been significant oxidation of these reduced gases. Despite these caveats, and if the assumption is correct that CH_4 is derived to a large extent from deeper locations in the system and have attained and preserved some sort of chemical equilibrium, we obtain temperatures of about 200 to 260°C applying the commonly used geothermometer of Norman and Bernhardt (1981). These temperatures are somewhat consistent with CH_4-CO_2 temperatures obtained from gas samples collected at springs which generally are considered more reliable because springs have a more direct access to deeper hydrothermal fluids.

Arnorsson developed geothermometers that use CO_2 or H_2 which are assumed to be derived from a liquid phase at depth coupled with N_2 and Ar which are of atmospheric origin. The geothermometer is principally based on the premise that N_2 and Ar solubility depends on temperature and is in equilibrium with the liquid phase at depth (Arnórsson et al., 1988). Using these geothermometers, again cautiously, given constraints discussed above, gives values from ambient to about 140°C CO_2/N_2 geothermometer (Diagram 2). The H_2/Ar geothermometer gives a wider temperature range from ambient to about 110°C. It is important to note that the temperature estimates using CO_2/N_2 and H_2/Ar in most cases is not consistent (Diagram 3). For most cases, the CO_2/N_2 temperatures are higher. The samples that show good agreement between the two geothermometers are probably the most reliable for providing an accurate temperature estimate for fluids at depth. These are DER-3, DER-4, DER-10, DER-11, and DEG-4. The range for these most consistent samples is about 50°C to 90°C. The best agreement of the higher temperature samples is DEG-1A.

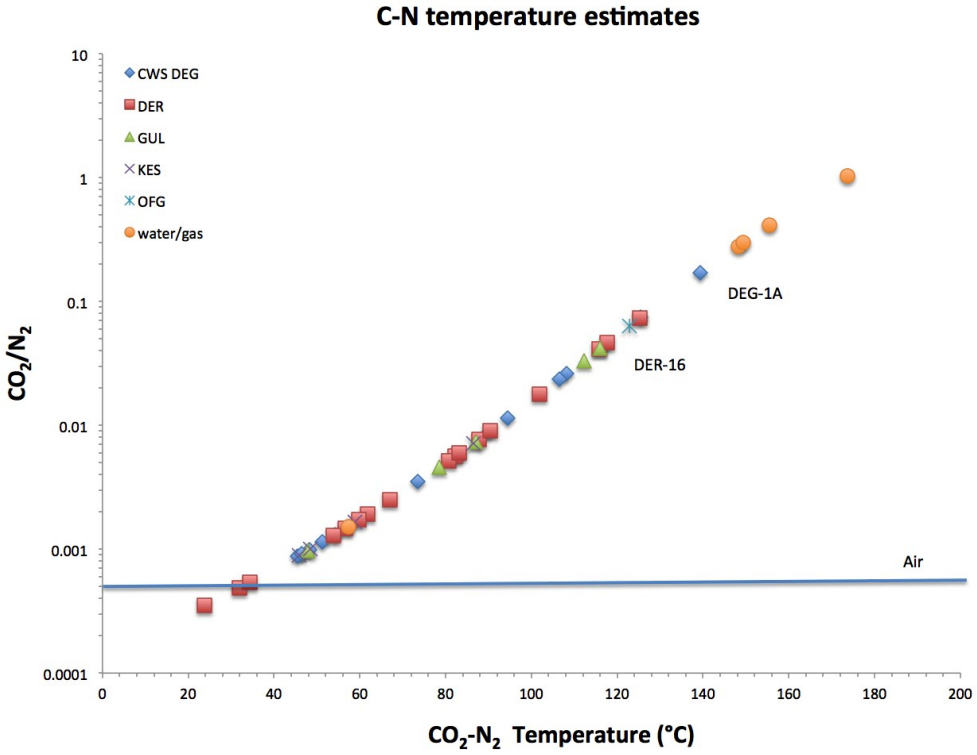

Diagram 2: relationship between CO2/N2 ratio and the resulting temperature using the CO2-N2 geothermometer of (Arnórsson et al., 1988)

In terms of the most promising area for further exploration and higher density of sampling, the areas close to the most recent lava flows and extensive fault traces, i.e., in the central part of the Degirmenler Concession are selected. In particular the area around sample DEG-1A should be explored further by sampling along and across the fault traces. Sample DEG-1A has the highest contribution of crustal/mantle CO_2 of all soil gas samples (Diagram 4), the highest CO_2/N_2 temperature (Diagram 5) and the best agreement between all applied geothermometers with CO_2/N_2 and N_2/H_2 giving a range of 120°C to 140°C and CH_4/CO_2 a significantly higher temperature of 260°C, which should be treated with caution because it is over 100°C higher than the two other and more consistent geothermometers.

6.2 Structural and Petrographic Conclusions

Detailed structural and petrographic mapping surveys suggest that the pathways for fluids and gases exist along the NW-SE trending faults; particularly on the areas where two or more faults intersect. The presence of thermal springs, and elevated geothermometers from gas chemistry corroborate these findings. However, as these features do not behave consistently, the degree of fracture based permeability remains questionable.

7. FINAL CONCLUSIONS

Using innovative technics along with the classic geothermal exploration methods has given insights into constraining the exploration targets in blind geothermal settings. The MMR technique may become a prerequisite for the future geothermal exploration studies. A further sequence of small grid MMR sampling in the most promising area could further establish the controls on pathways for fluid and gas.

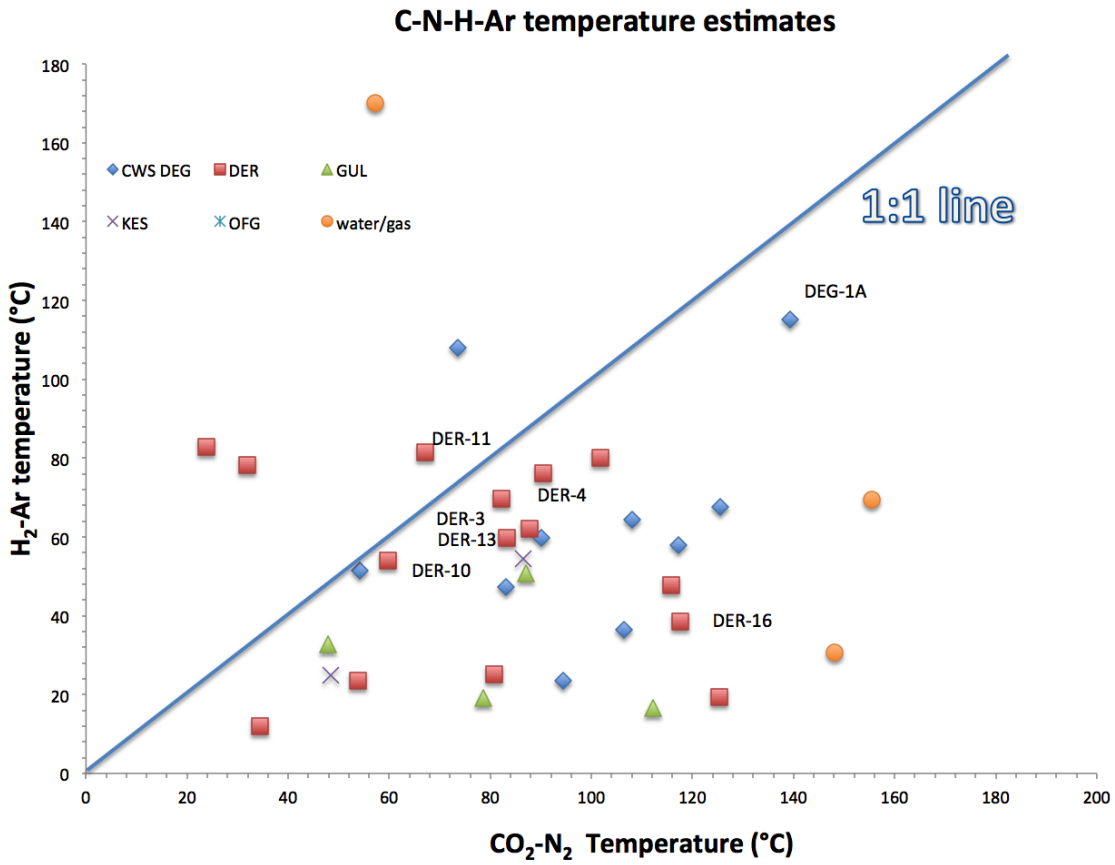

Diagram 3: Comparison of H2-Ar and CO2-N2 geothermometer (Arnórsson et al., 1988) temperature estimates

REFERENCES

Alici, P., Temek, A., and Gourgard. A., 2002. PB-Nd-Sr Isotope and Trace Element Geochemistry of Quaternary Extension–related Alkaline Volcanism: a Case Study of Kula Region (Western Anatolia, Turkey), Journal of Volcanology and Geothermal Research, 115, pp 487-510.

Arnórsson, S., Fridriksson, T. and Gunnarsson, I., 1998. Gas chemistry of the Krafla Geothermal Field, Iceland. In G.B. Arehartand J.R. Hulston (eds.) *Water-rock Interaction*, 613-616. Rotterdam: Balkema.

Dyer, J., 1987. Petrology of the Kula Volcanic Field Western Turkey, Master Thesis State University of New York at Albany, Master Thesis

Ersoy, Y. E., Helvaci, C., Sozbilir, H., 2010. Tectono-Stratigraphic Evolution of the NE–SW-Trending Superimposed Selendi Basin: Implications for late Cenozoic Crustal Extension in Western Anatolia, Turkey, Tectonophysics 488 (2010) 210–232.

Faulds, J. E., Bouchot, V. Moeck, I., and Oguz, K., 2009. Structural Controls on Geothermal Systems in Western Turkey: A Preliminary Report, GRC Transactions. Vol. 33. 2009.

Ferretti, A., Massonet, D., Monti Guarnieri, A., Prati, C. and Rocca, F. 2007. InSAR Principles: Guidelines for SAR Interferometry Processing and Interpretation, ESA TM-19 Gulec, N., Hilton, D.R., Mutlu, H., 2002. Helium Isotope Variations in Turkey: Relationships to Tectonics, Volcanism and Recent Seismic Activities, Chemical Geology, 187, pp. 129-142.

Graham, D.W., 2002. Noble gas isotope geochemistry of Mid-Ocean Ridge and Ocean Island Basalts: Characterization of mantle source regions. In: D. Porcelli, C. Ballentine, R. Wieler (eds.), MSA Special Volume: Noble Gases., 47: 247-317.

Isik, V., Seyitoglu, G., Cemen, L., 2003: Ductile-brittle Transition Along the Alasehir Detachment Fault and its Structural Relationship with the Simav Detachment Fault, Menderes Massif, Western Turkey, Tectonophysics 374, 1-18.

Norman, D.I. and Bernhardt, C.A., 1981. Assessment of geothermal reservoirs by analysis of gases in geothermal reservoirs: Final technical report, New Mexico energy institute, New Mexico State University, Las Cruces, 130 pp.

Tokcaer, M. and Savascin, M. Y., 2007. Tectono-Thermal Modeling Of Geothermal Systems and Boron Isotope Ratios in Geothermal Waters of Western Anatolia, Proceedings European Geothermal Congress 2007, Unterhaching, Germany, 30 May-1 June 2007.